Effect of accumulators on cavitation surge in hydraulic systems

Donghyuk Kang, Satoshi Yamazaki, Shusaku Kagawa, Byungjin An, Motohiko Nohmi, Kazuhiko Yokota

Effect of accumulators on cavitation surge in hydraulic systems

Donghyuk Kang[1]*, Satoshi Yamazaki[1], Shusaku Kagawa[2], Byungjin An[2], Motohiko Nohmi[2], Kazuhiko Yokota[1]

ISROMAC 2016

International Symposium on Transport Phenomena and Dynamics of Rotating Machinery

Hawaii, Honolulu

April 10-15, 2016

Abstract

The analysis of cavitation surge was performed to investigate the effect of accumulators on cavitation surge. The accumulator was modeled by using the momentum equation with a mass and a damping and a stiffness coefficients. The mass, damping and stiffness coefficients were associated with a pipe length between an accumulator and a main pipe, a valve resistance and a compliance of fluid in an accumulator, respectively. The upstream accumulator with the valve resistance had the stability effect and caused the increase of the angular velocity of cavitation surge. The downstream accumulator had the stability effect at small mass flow gain factors and caused the increase/ decrease of the angular velocity of cavitation surge at low/ large cavitation compliances. The amplitudes of flow and pressure oscillations can be reduced by the installation of the upstream accumulator.

Keywords

Cavitation surge — Lump parameter models — Accumulator

[1] *Department of Mechanical engineering, University of Aoyama Gakuin, Kanagawa, Japan*

[2] *Fluid Machinery at Systems Company, EBARA Corporation, Chiba, Japan*

***Corresponding author**: kang@me.aoyama.ac.jp

INTRODUCTION

Since cavitation surge is caused by the interaction of cavitation with hydraulic systems [1], an installation of an accumulator in hydraulic systems is planned for suppression of cavitation surge.

To predict the effect of accumulators on cavitation surge, the stability analysis of cavitation surge was performed for the hydraulic systems. The hydraulic systems consisted of an upstream tank, an inlet pipe, an upstream accumulator, a cavitating pump, a downstream pipe, an outlet pipe, a downstream accumulator, an outlet pipe and a downstream tank.

The effect of the accumulators was qualitatively discussed in the ranges of mass flow gain factor and cavitation compliance shown in the experiments [2, 3, 4, 5].

NOMENCLATURE

A^* : cross sectional area [m^2]

c : dimensionless compliance = $\dfrac{v}{\gamma\overline{\psi}}$ [-]

D^* : diameter of impeller [m]

K : cavitation compliance [-]

l : dimensionless pipe length $=l^*/D^*$ [-]

l^* : pipe length [m]

l_p : dimensionless chord length of impeller $=l_p^*/D^*$ [-]

l_p^* : chord length of impeller [m]

M : mass flow gain factor [-]

p^* : pressure [Pa]

p_{td}^* : total pressure at pump downstream [Pa]

p_{tu}^* : total pressure at pump upstream [Pa]

Q^* : flow rate [m^3/s]

R_p : flow gain [-]

S_p : pressure gain [-]

t : dimensionless time $=t^*\times U^*/D^*$ [-]

t^* : time [s]

U^* : tip velocity of impeller [m/s]

v : dimensionless fluid volume = $\dfrac{v^*}{A^*D^*}$ [-]

v^* : fluid volume [m^3]

γ : specific heat ratio [-]

ζ : valve resistance [-]

λ : pipe loss coefficient [-]

ρ^* : density of working fluid [m^3/s]

σ_u : cavitation number $=2(p_u^*-p_v^*)/\rho^*U^{*2}$ [-]

ϕ : flow coefficient $=Q^*/\rho^*U^{*2}$ [-]

ψ : dimensionless pressure $=2p^*/\rho^*U^{*2}$ [-]

ω : dimensionless complex angular velocity $=\omega^*D^*/U^*$[-]

ω^* : complex angular velocity [m/s]

ω_I : damping rate [-]

ω_R : angular velocity [-]

Superscript

- : time averaged component

^ : fluctuating component

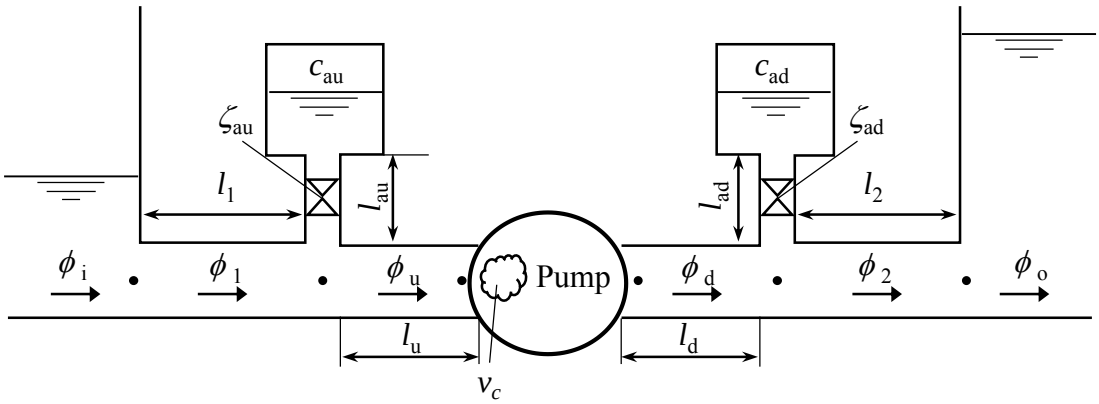

Figure 1. Schematic of the analytical model in the present study

Subscript

1 : inlet pipe
2 : outlet pipe
ad : downstream accumulator
au : upstream accumulator
c : cavitation
d : downstream pipe
i : upstream tank
o : downstream tank
u : upstream pipe

1. METHODS

The dynamic of hydraulic systems were treated in terms of lumped-parameter models [6, 7] which simplifies the description of the physical effects between two measuring points. The lump-parameter model is usally considered valid when the dimensions of a hydralic system are shorter than the acoustic wave length at the considered frequency.

For simplicity of the analytical model, the following assumuptions are adopted in the present analysis.

(1) The flow is one-dimensional.
(2) The flow and pressure oscillations are expressed as a temporally harmornic oscillation and infinitesimal. Thus, the second or higher order quantities are negligible.
(3) The working fluid is incompressible. The pressure loss is considered as the loss coefficient.
(4) The elastic deformation of all pipes is negligible and the cross-sectional area of a pipe is constant.
(5) The compliance of tanks is large and thus the pressure oscillation inside tanks is negligible.
(6) The cross-section area of all pipes connected to a main pipe from an accumulator is the same as the horizontal section area of accumulators.

Under the above assumptions, the dimensionless pressure and flow oscillations can be written in the complex form as follows.

$$\psi(t) = \overline{\psi} + \hat{\psi} e^{j\omega t},\ \ \phi(t) = \overline{\phi} + \hat{\phi} e^{j\omega t} \tag{1}$$

Here, $\overline{\psi} = 2\overline{p}^* / \rho^* U^{*2}$ and $\overline{\phi} = \overline{Q}^* / A^* U^*$ are the steady pressure and flow coefficients, respectively. $\hat{\psi} = 2\hat{p}^* / \rho^* U^{*2}$ and $\hat{\phi} = \hat{Q}^* / A^* U^*$ are the complex amplitudes of the unsteady pressure and flow coefficients, respectively. $t = t^* \times U^* / D^*$ is the dimensionless time and $\omega = \omega^* \times D^* / U^*$ is the dimensionless angular frequency. A^* is the cross-sectional area at the suction pipe and D^* is the diameter of the impeller. ω^* is the angular velocity and U^* is the tip velocity of the impeller. ρ^* is the density of the working fluid and j is the imaginary unit.

First, we consider the flow through the pipes shown in Fig.1. By putting Eq.(1) into the dimensionless unsteady continuity and momentum equations and subtracting the steady terms of them from themselves, the following equations can be introduced.

$$\hat{\phi}_i = \hat{\phi}_u \tag{2}$$

$$\hat{\phi}_2 = \hat{\phi}_o \tag{3}$$

Table 1. Default analytical parameters

Inlet pipe length, l_1	10
Upstream pipe length, l_u	3
Downstream pipe length, l_d	3
Outlet pipe length, l_2	30
Chord length of a impeller, l_p	0.3
Flow rate, $\overline{\phi}$	0.0577
Pipe loss coefficients, λ_1=λ_u=λ_d=λ_2	0.01
Flow gain, R_p	-10
Pressure gain, S_p	0
Compliance of accumulator, c	100

$$\hat{\psi}_i = -2\lambda_1 l_1 \overline{\phi}\hat{\phi}_1 - 2j\omega l_1 \hat{\phi}_1 \tag{4}$$

$$\hat{\psi}_u = \hat{\psi}_1 - 2\lambda_u l_u \overline{\phi}\hat{\phi}_u - 2j\omega l_u \hat{\phi}_u \tag{5}$$

$$\hat{\psi}_2 = \hat{\psi}_d - 2\lambda_d l_d \overline{\phi}\hat{\phi}_d - 2j\omega l_d \hat{\phi}_d \tag{6}$$

$$\hat{\psi}_2 = 2\lambda_u l_u \overline{\phi}\hat{\phi}_u + 2j\omega l_u \hat{\phi}_u \tag{7}$$

Here, the subscripts i, u, 1, d, 2, o indicate the inlet tank, the inlet pipe, the upstream pipe, the downstream pipe, the outlet pipe and the outlet tank, respectively. λ is the loss coefficient. $l = l^*/D$ is the dimensionless pipe length. The first and second terms of the right side in Eq.(4) indicate the hydraulic resistance and inertance, respectively.

Next, we consider the flow through the accumulator shown in

Fig.1. The momentum equations of the accumulator can be expressed as

$$\hat{\psi}_1 - 2l_{au} j\omega\hat{\phi}_{au} - 2\zeta_{au}\hat{\phi}_{au} = \hat{\psi}_{au}, \quad (8)$$

$$\hat{\psi}_2 - 2l_{ad} j\omega\hat{\phi}_{ad} - 2\zeta_{ad}\hat{\phi}_{ad} = \hat{\psi}_{ad}. \quad (9)$$

Here, ζ is the valve resistance. The subscripts au and ad indicate the upstream and downstream accumulators, respectively. The continuous equations for the accumulators can be expressed as

$$\hat{\phi}_u - \hat{\phi}_1 = \hat{\phi}_{au}, \quad (10)$$

$$\hat{\phi}_2 - \hat{\phi}_d = \hat{\phi}_{ad}. \quad (11)$$

With respect to the fluid inside the accumulators, the flow coefficients $\hat{\phi}_{au}$ and $\hat{\phi}_{ad}$ can be obtained as following equations.

$$\hat{\phi}_{au} = -j\omega\frac{v_{au}}{\gamma\overline{\psi}_{au}}\hat{\psi}_{au} = -c_{au} j\omega\hat{\psi}_{au} \quad (12)$$

$$\hat{\phi}_{ad} = -j\omega\frac{v_{ad}}{\gamma\overline{\psi}_{ad}}\hat{\psi}_{ad} = -c_{ad} j\omega\hat{\psi}_{ad} \quad (13)$$

Here, $v = v^*/A^*D^*$ is the dimensionless fluid volume of the accumulator. γ is the specific heat ratio and c is called the compliance.

By putting Eqs.(12) and (13) in Eqs.(8) and (9), the momentum equations with the mass and damping and stiffness coefficients were introduced as follows.

$$2l_{au}\omega^2\hat{\psi}_{au} - 2\zeta_{au} j\omega\hat{\psi}_{au} + \frac{1}{c_{au}}(\hat{\psi}_{au} - \hat{\psi}_1) = 0 \quad (14)$$

$$2l_{ad}\omega^2\hat{\psi}_{ad} - 2\zeta_{ad} j\omega\hat{\psi}_{ad} + \frac{1}{c_{ad}}(\hat{\psi}_{ad} - \hat{\psi}_2) = 0 \quad (15)$$

The mass, damping and stiffness coefficients corresponding to the first, second and third terms of the left sides are associated with the pipe length, the valve resistance and the compliance of fluid, respectively. These parameters will be examined in the present study.

A cavity volume v_c^* is assumed to be formed upstream of the cavitating pump. Then, the dimensionless continuity equation can be expressed as

$$\phi_d(t) - \phi_u(t) = \frac{dv_c(t)}{dt}. \quad (16)$$

Here, $v_c = v_c^*/A^*D^*$ is the dimensionless cavity volume. The change of the cavity volume dv_c can be considered to be functions of the upstream cavitation number

$$\sigma_u = 2(p_u^* - p_v^*)/\rho^* U^{*2} \quad (17)$$

and the upstream flow coefficient

$$\phi_u = Q_u/AU. \quad (18)$$

Thus, it can be written as

$$dv_c = \left(\frac{\partial v_c}{\partial\phi_u}\bigg|_{\sigma_u} d\phi_u + \frac{\partial v_c}{\partial\sigma_u}\bigg|_{\phi_u} d\sigma_u\right) = \left(-Md\phi_u - Kd\sigma_u\right) \quad (19)$$

where M and K are mass flow gain factor and cavitation compliance, respectively.

The pressure rise supplied from the cavitating pump can be expressed as the total pressure rise coefficient. The total pressure rise coefficient is defined as

$$\psi_p = 2(p_{td} - p_{tu})/\rho U^2. \quad (20)$$

Here. p_{tu} and p_{td} are the total pressures at the upstream of the cavitating pump and the downstream of the cavitating pump, respectively. Using the Bernoulli equation with the pressure rise of the cavitating pump, the following equation is obtained.

$$\hat{\psi}_d - \hat{\psi}_u = \hat{\psi}_p - \bar{\phi}\left(\hat{\phi}_d - \hat{\phi}_u\right) - j\omega l_p\hat{\phi}_d \quad (21)$$

Here, $l_p = l_p^*/D^*$ is the dimensionless inertial length of the cavitating pump. l_p^* is the mean value of the chord length. The first term of the right side indicates the unsteady total pressure rise of the cavitating pump. The second term of the right side shows the unsteady dynamic pressure rise. The last term of the right side indicates the inertia term.

The pressure rise of the cavitating pump $\hat{\psi}_p$ can be considered to be functions of the upstream cavitation number σ_u and the discharge flow coefficient ϕ_d on the assumption that cavitation occurs at the upstream of the cavitating pump and that the total pressure rise depends on the discharge flow rate. Thus, we can represent the unsteady pressure rise as

$$\hat{\psi}_p = \left(\frac{\partial\psi_p}{\partial\phi_d}\bigg|_{\sigma_u}\hat{\phi}_d + \frac{\partial\psi_p}{\partial\sigma_u}\bigg|_{\phi_d}\hat{\sigma}_u\right) = \left(R_p\hat{\phi}_d + 2S_p\hat{\psi}_u\right). \quad (22)$$

Here, R_p and S_p are called flow gain and pressure gain in the present study, respectively.

From above formulations, we obtained the homogeneous linear equations. The homogeneous linear equations have the complex angular frequencies expressed as

$$\omega = \omega_R + \omega_I. \quad (23)$$

Here, ω_R and ω_I show the angular velocity and the damping rate, respectively. For $\omega_I < 0$, the infinitesimal amplitude grow, which means cavitation surge. The zero damping rate indicates the onset boundary of cavitation surge.

Table 1 shows the tested parameters. These parameters are used in the present paper as the default parameters.

2. RESULTS AND DISCUSSION

Figure 2(a) shows the stability map of cavitation surge with the upstream accumulator for various compliances c_{au} with ζ_{au}=0 and l_{au}=0. The abscissa and the ordinate show mass flow gain factor and cavitation compliance, respectively. The upper and lower regions of the onset boundary of cavitation surge indicate the stable and cavitation surge regions, respectively. All results show that the lines, the onset boundaries of cavitation surge, indicate the positive slope. That is, the increase of cavitation compliance has the stabilizing effect and the increase of the mass flow gain factor causes cavitation surge.

Point A is located in the upper region of the onset boundary of cavitation surge for c_{au}=0. This means that the state of Point A is stable. As c_{au} is increased up to 100, Point A is located in the lower region of the onset boundary of cavitation surge and thus its state becomes cavitation surge. Assuming that cavitation compliance and mass flow gain factor are not changed by the modification of the hydraulic systems in the present study, we can say that the upstream accumulator has the instability effect. For c_{au}=1, the cavitation surge region is more widened than that for c_{au}=100.

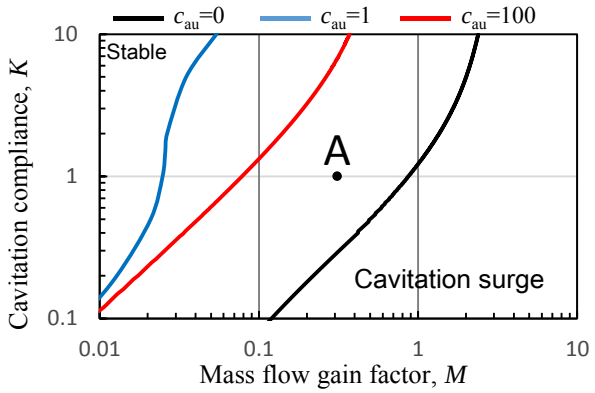

(a) Onset condition of cavitation surge

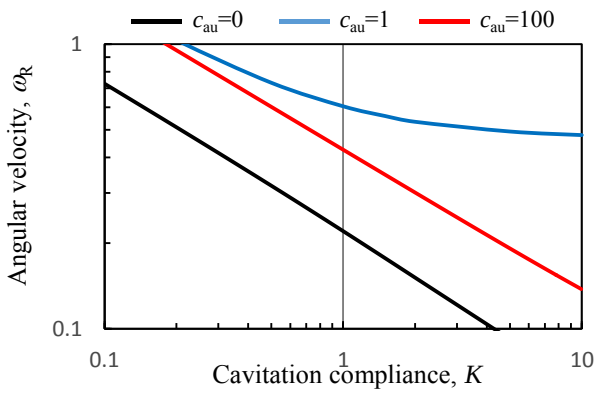

(b) Angular velocity

Figure 2. Onset condition of cavitation surge and angular velocity for the upstream accumulator with ζ_{au}=0 and l_{au}=0

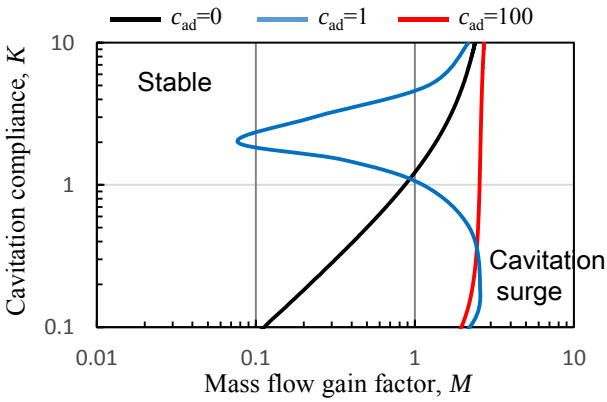

(a) Onset condition of cavitation surge

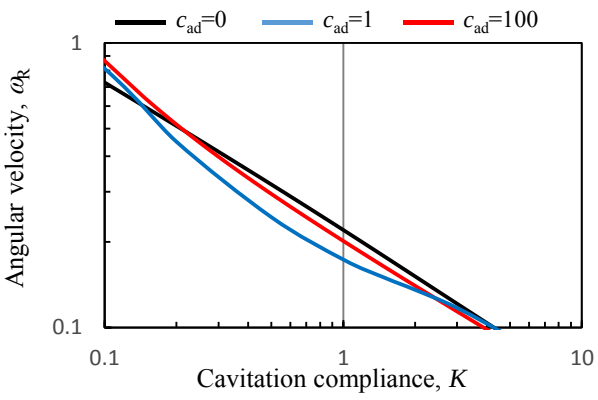

(b) Angular velocity

Figure 3. Onset condition of cavitation surge and angular velocity for the downstream accumulator with ζ_{ad}=0 and l_{ad}=0

Figure 2(b) shows the angular velocities at the onset boundary of cavitation surge with the upstream accumulator for various compliances c_{au} with ζ_{au}=0 and l_{au}=0. The horizontal and vertical axes represent cavitation compliance and the angular velocity, respectively. All results show that angular velocity decreases with the increase of cavitation compliance. The upstream accumulator causes the increase of the angular velocity of cavitation surge. This is believed to be due to the decrease of the pipe length by the installation of the upstream accumulator. Namely, it says that the upstream accumulator acts as the inlet tank.

Figure 3(a) shows the stability map of cavitation surge with the downstream accumulator for various compliances c_{ad} with ζ_{ad}=0 and l_{ad}=0. For c_{ad}=100, the stable region is widened mainly at small mass flow gain factors as compared to the result for c_{ad}=0. Thus, the downstream accumulator has the stability effect at small mass flow gain factors. For c_{ad}=1, the onset boundary of cavitation surge at small mass flow gain factors is similar to that for c_{ad}=100 and the onset boundary of cavitation surge at large mass flow gain factors approaches to that for c_{ad}=0.

Figure 3(b) shows the angular velocities at the onset boundary of cavitation surge with the downstream accumulator for various compliances c_{ad} with ζ_{ad}=0 and l_{ad}=0. For c_{ad}=100 and c_{ad}=1, the angular velocities increases/ decrease at small/ large cavitation compliances. This is different from the result of the upstream accumulator that the angular velocity increases at all cavitation compliances.

Figure 4(a) shows the stability map of cavitation surge with the upstream accumulator for various resistances ζ_{au} with c_{au}=100 and l_{au}=0. For ζ_{au}=0.5, the onset boundary of cavitation surge is shifted to the cavitation surge. This indicates that the stable region becomes large and that the upstream accumulator with the valve resistance has the stability effect. As the valve resistance is increased up to ζ_{au}=10.0, the onset boundary of cavitation surge at small mass flow gain factors is moved to the right side but the onset boundary of cavitation surge at large mass flow gain factors approaches to the result without the accumulator.

Figure 4(b) shows the angular velocities with the upstream accumulator for various resistances ζ_{au} with c_{au}=100 and l_{au}=0. For ζ_{au}=0.5, the angular velocity is slightly decreased at large cavitation compliances as compared to the result for ζ_{au}=0. For ζ_{au}=10, the angular velocity is almost the same as that without the accumulator.

Figure 5(a) shows the stability map of cavitation surge with the downstream accumulator for various valve resistances ζ_{ad} with c_{ad}=100 and l_{ad}=0. For ζ_{ad}=0.5, the onset boundary of cavitation surge is slightly shifted to the left side from that for ζ_{ad}=0. For ζ_{ad}=10, the onset boundary of cavitation surge at

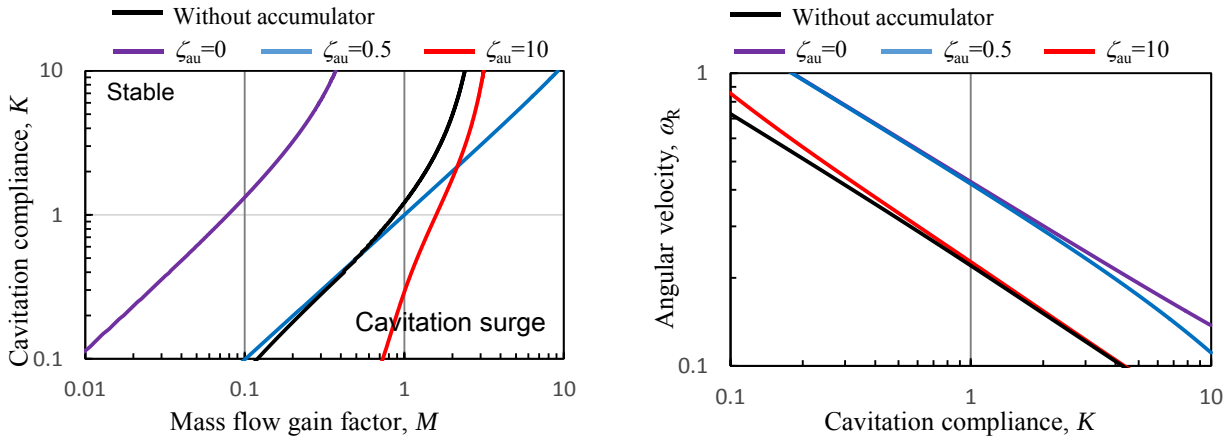

(a) Onset condition of cavitation surge **(b)** Angular velocity

Figure 4. Onset condition of cavitation surge and angular velocity for the upstream accumulator with c_{au}=100 and l_{au}=0

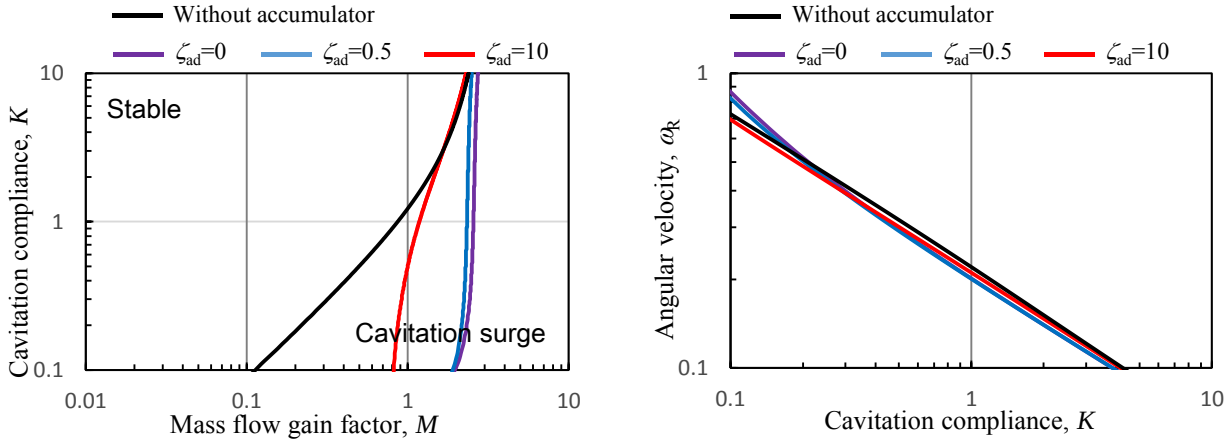

(a) Onset condition of cavitation surge **(b)** Angular velocity

Figure 5. Onset condition of cavitation surge and angular velocity for the downstream accumulator with c_{ad}=100 and l_{ad}=0

large mass flow gain factors approaches to the result without the accumulator. All results show that the valve resistance of the downstream accumulator has the instability effect.

Figure 5(b) shows the angular velocities with the downstream accumulator for various resistances ζ_{ad} with c_{ad}=100 and l_{ad}=0. The tendency, the increase/ decrease of the angular velocity at low/ large mass flow gain factors, is not changed by the valve resistance.

Figure 6(a) shows the stability map of cavitation surge with the upstream accumulator for various pipe lengths l_{au} with c_{au}=100 and ζ_{au}=0. For l_{au}=3, the stable region becomes large as compared to the result for l_{au}=0. For l_{au}=10, the stable region is more widened.

Figure 6(b) shows the angular velocity of cavitation surge with the upstream accumulator for various pipe lengths l_{au} with c_{au}=100 and ζ_{au}=0. For l_{au}=3, the angular velocity is smaller than the result for l_{au}=0. For l_{au}=10, the angular velocity becomes smaller.

Figure 7(a) shows the stability map of cavitation surge with the downstream accumulator for various pipe lengths l_{ad} with c_{ad}=100 and ζ_{ad}=0. For l_{ad}=3, the cavitation surge region increases as compared to the result for l_{ad}=0. For l_{ad}=10, the cavitation surge region at low mass flow gain factors becomes larger. All results of Figs 3(a), 5(a) and 7(a) show that the onset boundary of cavitation surge at large mass flow gain factors is not affected by the downstream accumulator.

Figure 7(b) shows the angular velocities of cavitation surge with the downstream accumulator for various pipe lengths l_{ad} with c_{ad}=100 and ζ_{ad}=0. As shown in Figs.3(b) and 5(b), the angular velocity increase/decrease at low/large mass flow gain factors. We observed the intersections of the lines for l_{ad}=0, l_{ad}=3 and l_{ad}=10 and the line without the accumulator. The intersections for l_{ad}=0, l_{ad}=3 and l_{ad}=10 are shown by ①, ② and ③, respectively. As l_{ad} is increased, the cavitation compliance of the intersection increases.

Figure 8 shows the amplitude ratios and phases of the flow and pressure oscillations with the upstream accumulator. The three cases were examined. The first case is without the accumulator, the second case is with the upstream accumulator for c_{au}=100 ζ_{au}=0 and l_{au}=0 and the final case is with the upstream accumulator for c_{au}=100 ζ_{au}=10 and l_{au}=0. Without the accumulator, the amplitudes of ϕ_l and ϕ_u are larger than those of ϕ_d and ϕ_2 as shown in Fig.8(a) and the phases of ϕ_d and ϕ_2 are about -35 degrees as shown in Fig.8(b). However, the amplitudes of all pressure oscillations

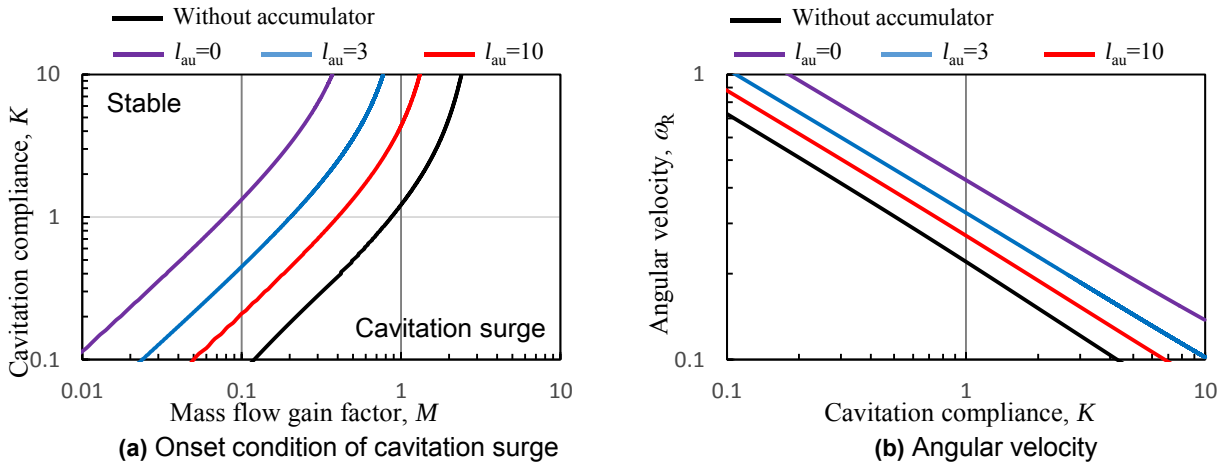

(a) Onset condition of cavitation surge **(b)** Angular velocity

Figure 6. Onset condition of cavitation surge and angular velocity for the upstream accumulator with c_{au}=100 and ζ_{au}=0

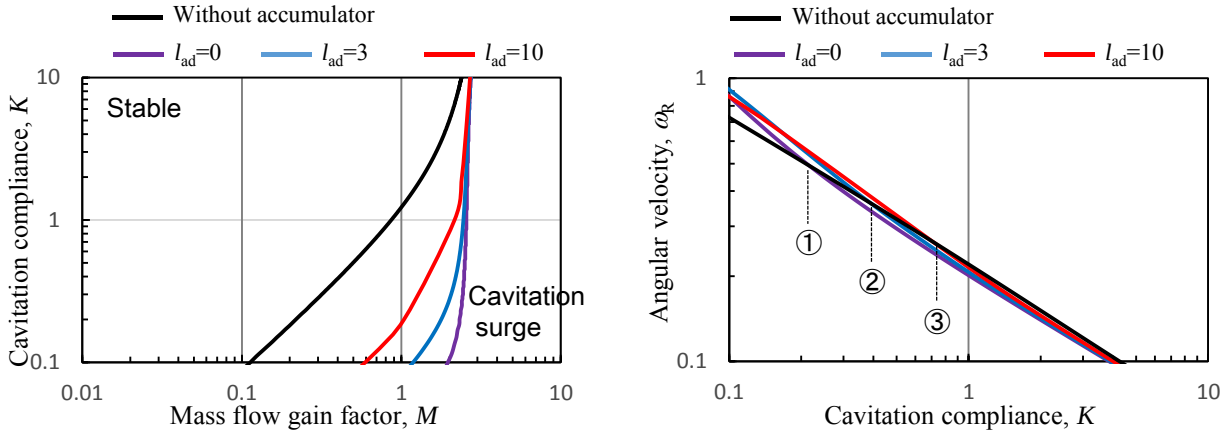

(a) Onset condition of cavitation surge **(b)** Angular velocity

Figure 7. Onset condition of cavitation surge and angular velocity for the downstream accumulator with c_{ad}=100 and ζ_{ad}=0

are almost equal and nearly 5 times higher than the amplitude of ϕ_u as shown in Fig.8(c). It can be observed that the phase differences between the pressure and flow oscillations are about -90 degrees due to the inertia effect as shown in Fig.8(d). For c_{au}=100 ζ_{au}=0 and l_{au}=0, the amplitudes of ϕ_1, ϕ_d and ϕ_2 and all pressure oscillations are very lower than the amplitude of ϕ_u. This indicates that the amplitudes of the flow and pressure oscillations can be reduced by the installation of the upstream accumulator. The phases of ϕ_d and ϕ_2 are about 25 degrees. For c_{ad}=100 ζ_{ad}=10 and l_{ad}=0, all magnitudes and phases are similar to the results without the accumulator except for the phase of ψ_u.

Figure 9 shows the amplitude ratios and phases of the flow and pressure oscillations with the downstream accumulator. For c_{ad}=100 ζ_{ad}=0 and l_{ad}=0, the amplitudes of ϕ_d and ϕ_2 are slightly larger than those without the accumulator as shown in Fig.9(a). This result shows that the flow induced from the change of the cavity volume easily flows to the downstream of the cavitating pump. The phases of ϕ_d and ϕ_2 are about 84 degrees as shown in Fig.9(b). The amplitudes of ψ_d and ψ_2 are largely decreased as compared to those without the downstream accumulator as shown in Fig.9(c). All result show that the upstream flow and pressure oscillations are not sinigificantly affected by the downstream accumulator. For c_{ad}=100 ζ_{ad}=10 and l_{ad}=0, the ampliutudes and phases of the pressure and flow oscillations are similar to the results without the accumulator.

3. CONCLUSION

The effects of the accumulators on cavitation surge based on the one dimensional linear stability analysis by the lump-parameter models were investigated. The following conculusions are obtained.

(1) The upstream accumulator with the small valve resistance has the stability effect and causes the increase of the angular velocity.

(2) The downstream accumulator at low mass gain factors has the stability effect and causes the increase/ decrease of the angular velocity at low/ large cavitation compliances.

(3) The valve resistance of the downstream accumulator has the instability effect at low mass flow gain factors.

(4) The onset boundaries of cavitation surge at large mass flow gain factors are not affected by the downstream accumulator.

(5) The amplitudes of the flow and pressure oscillations can

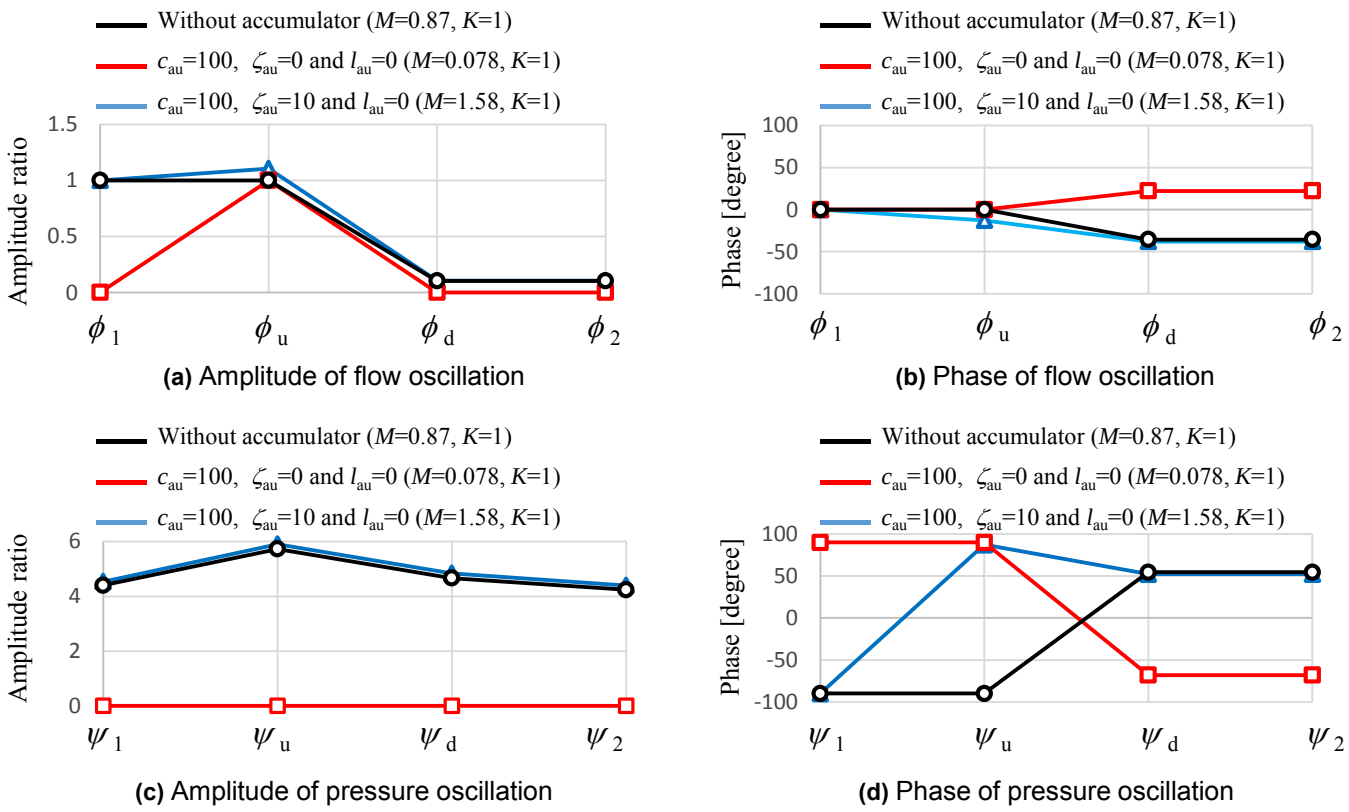

(a) Amplitude of flow oscillation

(b) Phase of flow oscillation

(c) Amplitude of pressure oscillation

(d) Phase of pressure oscillation

Figure 8. Amplitude ratios and phases of the flow and pressure oscillations for the upstream accumulator

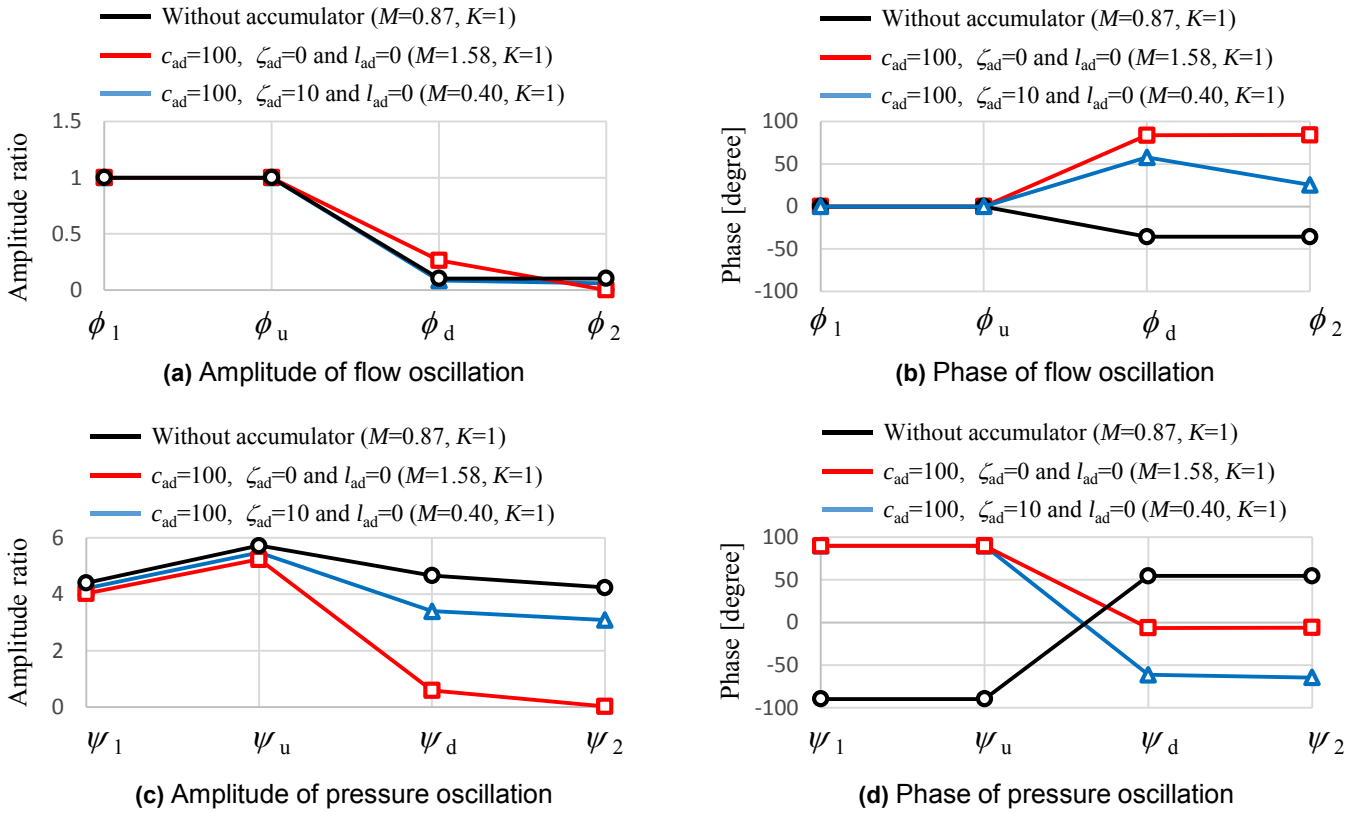

(a) Amplitude of flow oscillation

(b) Phase of flow oscillation

(c) Amplitude of pressure oscillation

(d) Phase of pressure oscillation

Figure 9. Amplitude ratios and phases of the flow and pressure oscillations for the downstream accumulator

be reduced by the installation of the upstream accumulator.

(6) The flow induced from the change of the cavity volume easily flows to the downstream of the cavitating pump by the installation of the downstream accumulator.

(7) The upstream flow and pressure oscillations are not sinigificantly affected by the downstream accumulator.

We are preparing the experiment to investigate the effect of

the accumulators on cavitation surge observed in an double suction centrifugal pumps [8]. The upstream and the downstream accumulators with the valve resitances are effective for avoidance of cavitation surge.

REFERENCES

[1] W.E. Young. Study of Cavitating Inducer Instabilities. Final Report NASA-CR-123939, 1972.

[2] C.E. Brennen. The Bubbly Flow Model for the Dynamic Characteristics of Cavitating Pump. Journal of Fluid Mechanics, 89, pp.223~240, 1978.

[3] S. Rubin. An Interpretation of Transfer Function Data for a Cavitating Pump. 40th AIAA/ASME/SAE/ASEE Joint Propulsion Conference AIAA-2004-4025, 2004.

[4] K. Yonezawa. J. Aono. D. Kang. H. Horiguchi. Y. Kawata. Y.Tsujimoto. Numerical Evaluation of Dynamic Transfer Matrix and Unsteady Cavitation Characteristics of an Inducer. International Journal of Fluid Machinery and System. 5, pp.126~133, 2012.

[5] D. Kang. S. Hatano. K. Yokota. S. Kagawa. M. Nohmi. Estimation of the Dynamic Characteristics of a Double-Suction Centrifugal Pump in Cavitation Surge. Vol.3. pp.170-176, 2015 (in Japanese).

[6] A. Cervone. Y. Tsujimoto. Y. Kawata. Evaluation of the Dynamic Transfer Matrix of Cavitating Inducer by Means of a Simplified "Lumped-Parameter" Model. Journal of Fluid Mechanics Vol.131 pp.041103-1~.041103-9, 2009.

[7] D. Kang. K. Yokota. Analytical study of Cavitation Surge in Hydraulic system. Journal of Fluid Mechanics Vol.136 No.10. pp.101103-101113, 2014.

[8] S. Hatano. D. Kang. K. Yokota. S. Kagawa. M. Nohmi. Study of Cavitation Instabilities in Double Suction Centrifugal Pump. International Journal of Fluid Machinery and Systems. Vol.7. No.8. pp.94-100, 2014.